

# Nonconventional versus Conventional Application of Pseudo-First-Order Kinetics to Fundamental Organic Reactions

VERNON D. PARKER, WEIFANG HAO, ZHAO LI, RUSSELL SCOW

Department of Chemistry and Biochemistry, Utah State University, Logan, UT 84322-0300

Received 28 May 2011; revised 20 July 2011; accepted 20 July 2011

DOI 10.1002/kin.20609

Published online 26 September 2011 in Wiley Online Library (wileyonlinelibrary.com).

**ABSTRACT:** Three new analysis procedures for pseudo-first-order kinetics are introduced and applied to eight different fundamental organic reactions. The reactions belong to the following classes: nitroalkane proton transfer, formal hydride ion transfers from NADH model compounds, and  $S_N2$  reactions of alkyl halides with ionic and neutral nucleophiles. The three methods consist of (1) half-life dependence of  $k_{app}$ , (2) sequential linear pseudo-first-order correlation, and (3) revised instantaneous rate constant analysis. Each of the three procedures is capable of distinguishing between one- and multistep mechanisms, and the combination of the three procedures provides a powerful strategy for differentiating between the two mechanistic possibilities. The data from the eight reactions chosen as examples clearly show how the procedures work in practice. © 2011 Wiley Periodicals, Inc. *Int J Chem Kinet* 44: 2–12, 2012

## INTRODUCTION

In 1997, Professor George S. Hammond published a short article entitled “Physical Organic Chemistry after 50 Years: It Has Changed, but Is It Still There?” [1]. In this article, Hammond summarized the remarkable developments in the subdiscipline since it began with the work of Hammett [2]. No mention was made of the development of pseudo-first-order kinetic method, which

was the most important kinetic technique used by the vast majority of physical organic chemists. Aside from the development of very rapid kinetic techniques, essentially no improvements were made in the methods for which so many rate constants were measured for linear free-energy relationships. This is evident from the classic book *Kinetics and Mechanism*, by J. W. Moore and R. G. Pearson, published in 1981 [3]. This deficiency continued for the remainder of the 20th century. The digital revolution occurred during the time period of the development of physical organic chemistry. The latter had a great influence on the work of the physical chemists studying rapid kinetics but did not filter down to the physical organic chemists measuring rate constants of slower reactions. The objective

---

Correspondence to: Vernon D. Parker; e-mail: vernon.parker@usu.edu.

Contract grant sponsor: National Science Foundation.

Contract grant number: ARRA: CHE-0923654.

© 2011 Wiley Periodicals, Inc.

of our work is to fill the gap by introducing work on the fundamental reactions of organic chemistry using new methods, which take advantage of modern digital acquisition of absorbance–time data and extensive new data analysis of pseudo-first-order kinetics. During the current century, several papers have appeared that deal with inadequacy of a simple fit of an exponential curve to establish a simple one-step mechanism [4]. The work of Kormányos and coworkers [4b], entitled “Inherent Pitfalls in the Simplified Evaluation of Kinetic Curves,” is particularly relevant to the topic of this paper. A more mathematical approach is presented for the analysis of the kinetics of complex systems in [4c]. The work of Nagy and Turányi [4a] deals with the effect of uncertainties in rate constants on the reliability of the corresponding activation parameters.

The kinetic response of a wide variety of reactions will be covered without mechanism discussions. Instead we will present the results of the application of three different nonconventional pseudo-first-order procedures on the data. The data presented for each reaction result from a single set of stopped-flow experiments carried out over the course of one day. In all cases, the data presented are a minute fraction of the body of data available in our laboratory for each of these reactions, but at the same time are representative of the latter. The purpose of this type of presentation is to allow readers to assess the data without being influenced by the author’s views on the mechanistic implications of the data.

## EXPERIMENTAL METHODS AND DATA PROCESSING

The methods discussed are limited to three general procedures, and the first is a more detailed application of the conventional pseudo-first-order kinetic relationship in a way that in some cases clearly distinguishes between simple single-step and complex multistep mechanisms. When a complex mechanism is indicated, the other two procedures provide data, which give more details of the kinetic response and can verify that the reaction follows a complex mechanism. The methods are discussed using experimental data for the  $S_N2$  reaction of phenoxide ion with methyl iodide in acetonitrile at 298 K.

### Half-Life Dependence of Conventional Pseudo-First-Order Rate Constants

The procedure involves converting absorbance–time profiles (Abs–t) to  $-\ln(1 - ER)$ –time profiles, where

**Table I** Changes in the Slopes and the Intercepts with the Extent of Reaction during Conventional Pseudo-First-Order Analysis of the Reaction of Phenoxide Ion with Methyl Iodide in Acetonitrile at 298 K

$k_{app}$ ( $s^{-1}$ )	Intercept ( $s^{-1}$ )	Number of HL
0.0125	0.0116	0.5
0.0125	0.0123	1.0
0.0121	0.0223	2.0
0.0117	0.0445	3.0
0.0111	0.0832	4.0

ER is the extent of reaction. The latter are then subjected to linear least-squares analysis on five different segments of the data over time ranges corresponding to 0–0.5 half-lives (HL), 0–1 HL, 0–2 HL, 0–3 HL, and 0–4 HL. The data for the reaction of phenoxide ion (0.5 mM) with MeI (51.4 mM) in acetonitrile at 298 K are summarized in Table I. In this case, the data show that the values ( $0.0125 s^{-1}$ ) of the apparent pseudo-first-order rate constant ( $k_{app}$ ) over the first two data segments were identical within experimental error. Values obtained for longer segments of the data (1.0–4.0 HL) steadily decreased with degree of conversion. While the changes in  $k_{app}$  observed are modest, the corresponding changes in the zero-time intercepts are much larger and suggest that this parameter is much more sensitive to the deviations from first-order kinetics than  $k_{app}$  is. Obviously, the response expected for the single-step mechanism is a constant value of  $k_{app}$  and an intercept independent of the number of HL taken into the linear least-squares correlation.

### Sequential Pseudo-First-Order Linear Correlation

This analysis has been described in our recent papers [5–7]. The procedure involves recording 2000-point Abs–time profiles over about the first HL of the reaction. Linear least-squares analysis is then carried out over the following point segments: 1–11, 1–21, 1–31, 1–41, 1–51, 1–101, 1–201, . . . , 1–1901. This gives 24  $k_{app}$  values at the midpoints of the segments.

Standard deviations (SD) of the  $k_{app}$  evaluated for multiple (normally 20) stopped-flow shots are then recorded. The analysis is illustrated in Table II for the reaction of phenoxide ion with methyl iodide in acetonitrile at 298 K.

**Table II** Apparent Rate Constants and Standard Deviations Obtained by the 24-Point Sequential Analysis of the Reaction of Methyl Iodide with Phenoxide Ion in Acetonitrile at 298 K

Time (s)	$k_{app}$ ( $s^{-1}$ )	SD ( $s^{-1}$ )	Segment
0.14	0.0444	0.01016	1
0.27	0.0324	0.00433	2
0.40	0.0263	0.00191	3
0.53	0.0230	0.00117	4
0.66	0.0207	0.00081	5
1.31	0.0157	0.00034	6
2.61	0.0136	0.00015	7
3.91	0.0132	0.00007	8
5.21	0.0130	0.00006	9
6.51	0.0130	0.00005	10
7.81	0.0130	0.00005	11
9.11	0.0130	0.00005	12
10.41	0.0130	0.00005	13
11.71	0.0130	0.00005	14
13.01	0.0130	0.00005	15
14.31	0.0130	0.00005	16
15.61	0.0130	0.00005	17
16.91	0.0130	0.00005	18
18.21	0.0130	0.00005	19
19.51	0.0130	0.00005	20
20.81	0.0130	0.00006	21
22.11	0.0130	0.00006	22
23.41	0.0129	0.00006	23
24.71	0.0129	0.00006	24

The SD value for segment 1 is nearly 25% of the  $k_{app}$  value, and SD falls dramatically until it stabilizes to about 5% of the corresponding  $k_{app}$  from segments 8 to 24. The reason for the large SD in the early segments is related to the small number of points used in the linear correlations of the data in these segments. Each stopped-flow experiment is generally repeated at least three times. The expected result (20 shots) of the 24-point procedure for the single-step mechanism is a rate constant, independent of time and of the particular time segment analyzed.

Although the primary purpose of this method is to estimate the errors in  $k_{app}$ , the plot shown in Fig. 1 provides a convenient visual representation of the data, showing an initial high value and the subsequent decay to a plateau value as steady state is reached in about 2–3 s. The expected result of the 24-point procedure for the single-step mechanism is a rate constant, independent of time and of the particular time segment analyzed.

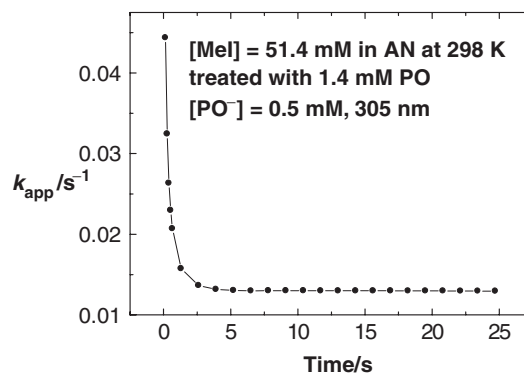


**Figure 1** Apparent rate constants ( $k_{app}$ )–time plot for the reaction between phenoxide ion and methyl iodide in acetonitrile at 298 K (1.0 HL = 48.6 s).

### A New Procedure for the Estimation of Instantaneous Rate Constant–Time Profiles

An obvious extension of the method discussed above is to include additional correlations. To do this, the points in the data segment are 1–3, 1–4, 1–5, 1–6, . . . , 1–2000, and a 1998-point array of  $k_{app}$ –time data is obtained. The procedure was applied to calculated  $-\ln(1 - ER)$ –time profiles, and the results were then compared to instantaneous rate constant ( $k_{inst}$ –time) profiles obtained at the midpoint between all points, as presented earlier [8]. The comparison showed that the  $k_{app}$ –time values at short times, as well as those near the end of the 1998-point array, were nearly identical to the corresponding  $k_{inst}$  values. The largest deviations (about 5%) were found in values near the center of the correlation. It was concluded that for all practical purposes the values obtained by the new procedure are equivalent to  $k_{inst}$  values, and the term  $k_{IRC}$  is appropriate to distinguish between the two different IRCs. The plot in Fig. 2 shows the application of the procedure outlined above.

## PROTON TRANSFER REACTIONS OF NITROALKANES

### Proton Transfer Reactions of the Simple Nitroalkanes

The well-known phenomenon referred to as the nitroalkane anomaly was named by Kresge [9] to describe the inverse relationship between the equilibrium and kinetic acidities of nitromethane, nitroethane, and 2-nitropropane (2-NP) in aqueous solution. Kresge, and all others who have studied these reactions, treated the data as arising from a simple single-step process.

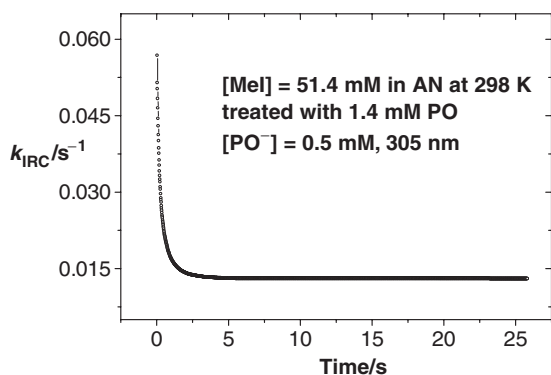
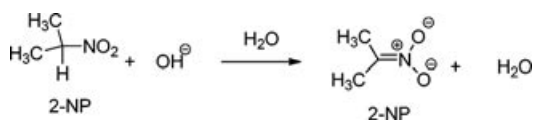


**Figure 2** Apparent IRC ( $k_{\text{IRC}}$ )–time plot for the reaction between phenoxide ion and methyl iodide in acetonitrile at 298 K (1.0 HL = 48.6 s).



**Scheme 1**

We have recently [6] reinvestigated the reactions and observed significant deviations from pseudo-first-order behavior. Here we take 2-NP as an example and show how detailed pseudo-first-order kinetics distinguish between single- and multistep mechanisms for the reactions of the simple nitroalkanes with hydroxide ion in water.

The HL dependence of  $k_{\text{app}}$  for the proton transfer reaction between 2-NP and hydroxide ion in water (Scheme 1) obtained by the application of the pseudo-first-order linear least-squares procedure is illustrated by the data given in Table III. Once again, the change in  $k_{\text{app}}$  as a function of number of HL analyzed is modest but the trend of decreasing rate constants with increases in the latter is significant and reproducible. The observed intercepts are much more sensitive to the

**Table III** Changes in the Slopes and the Intercepts with the Extent of Reaction during Conventional Pseudo-First-Order Analysis of the Reaction of 2-NP (0.2 mM) with Hydroxide Ion (100 mM) in Water at 298 K

$k_{\text{app}}$ ( $\text{s}^{-1}$ )	Intercept ( $\text{s}^{-1}$ )	Number of HL
0.0182	0.0017	0.5
0.0171	0.0104	1.0
0.0168	0.0178	2.0
0.0165	0.0270	3.0
0.0163	0.0404	4.0

**Table IV** Apparent Rate Constants and Standard Deviations Obtained by the 24-Point Sequential Analysis of the Reaction of 2-NP (0.2 mM) with Hydroxide Ion (100 mM) in Water at 298 K

Time (s)	$k_{\text{app}}$ ( $\text{s}^{-1}$ )	SD ( $\text{s}^{-1}$ )	Segment
0.14	0.0250	0.0045	1
0.25	0.0223	0.0013	2
0.36	0.0218	0.0012	3
0.47	0.0216	0.0008	4
0.59	0.0214	0.0006	5
1.15	0.0209	0.0002	6
2.27	0.0201	0.0002	7
3.40	0.0195	0.0002	8
4.52	0.0189	0.0002	9
5.65	0.0185	0.0002	10
6.77	0.0182	0.0002	11
7.90	0.0179	0.0002	12
9.02	0.0177	0.0002	13
10.15	0.0175	0.0002	14
11.27	0.0174	0.0002	15
12.40	0.0172	0.0002	16
13.52	0.0171	0.0002	17
14.65	0.0170	0.0002	18
15.77	0.0169	0.0002	19
16.90	0.0168	0.0002	20
18.02	0.0168	0.0002	21
19.15	0.0167	0.0002	22
20.27	0.0166	0.0002	23
21.40	0.0166	0.0002	24

deviations from first-order kinetics. The deviations of both of these quantities from that expected for first-order kinetics are a clear indication of the operation of a complex mechanism.

The 24-point sequential correlation of abs–time data over 1 HL (Table IV) for the reactions of 2-NP not only verifies the time dependence of  $k_{\text{app}}$  but also provides standard deviations of the latter for repetitive stopped-flow shots. As observed before, the SD are greatest for the initial  $k_{\text{app}}$  values but decrease steadily over the first six segments and then goes to a constant value equal to 1% or less of the corresponding  $k_{\text{app}}$ .

The IRC–time profile for product formation during the reaction of 2-NP (0.2 mM) with hydroxide ion (100 mM) in water (Fig. 3) sharply decreases from about  $0.03 \text{ s}^{-1}$  at short times to a more slowly decreasing profile near  $0.015 \text{ s}^{-1}$  at 1 HL. The expected result for the one-step mechanism is a straight line with zero slope, while that for a complex mechanism increases from zero at short times when only product absorbs at the experimental wavelength. On the other hand, an initial decreasing IRC–time profile at a wavelength the

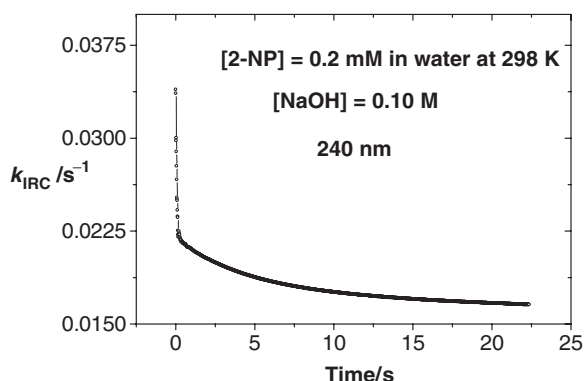


**Figure 3** Apparent IRC ( $k_{\text{IRC}}$ )-time plot for the reaction of 2-NP (0.2 mM) with hydroxide ion (100 mM) in water at 298 K (1.0 HL = 40.6 s).

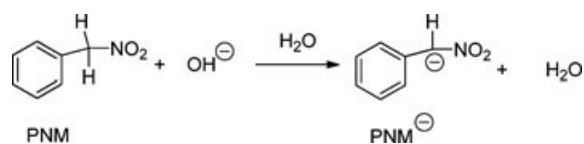
product but not the reactant absorbs indicates that a reaction intermediate is responsible for the initial sharp decrease in absorbance.

### Proton Transfer Reactions of Phenylnitroalkanes in Water

The proton transfer reactions of phenylnitromethane (PNM) in water and in water-DMSO mixture have been studied extensively by Bernasconi [10], and the results have played a prominent role in discussion of the principle of nonperfect synchronization [11]. A recent paper on proton transfer reactions of PNMs was concerned with the implications on the nitroalkane anomaly [12].

The conventional pseudo-first-order study of the reaction of PNM with hydroxide ion in water (Scheme 2) is illustrated by the data presented in Table V, in which  $k_{\text{app}}$  decreases steadily from 0.440 over 1 HL to  $0.356 \text{ s}^{-1}$ , while the intercept increased over the same range from  $-0.001$  to 0.136.

The 24-point sequential analysis shows more detail as illustrated in Table VI. The value of  $k_{\text{app}}$  in segment 1 was observed to be equal to 0.403, and then rises smoothly to a maximum value of 0.449 at segment 6 and then decreases steadily to  $0.434 \text{ s}^{-1}$  at segment 24.



**Scheme 2**

**Table V** Changes in the Slopes and the Intercepts with the Extent of Reaction during Conventional Pseudo-First-Order Analysis of the Reaction of PNM (0.0518 mM) with Hydroxide Ion (4.0 mM) in Water at 298 K

$k_{\text{app}} \text{ (s}^{-1}\text{)}$	Intercept ( $\text{s}^{-1}$ )	Number of HL
0.440	-0.001	0.50
0.433	0.001	1.00
0.420	0.012	2.00
0.398	0.043	3.00
0.356	0.136	4.00

**Table VI** Apparent Rate Constants and Standard Deviations Obtained by the 24-Point Sequential Analysis of the Reaction of PNM (0.0518 mM) with Hydroxide Ion (4.0 mM) in Water at 293 K

Time (s)	$k_{\text{app}} \text{ (s}^{-1}\text{)}$	SD ( $\text{s}^{-1}$ )	Segment
0.006	0.403	0.138	1
0.011	0.426	0.043	2
0.016	0.434	0.030	3
0.021	0.442	0.020	4
0.026	0.442	0.015	5
0.051	0.449	0.009	6
0.101	0.447	0.004	7
0.151	0.445	0.002	8
0.201	0.444	0.002	9
0.251	0.444	0.002	10
0.301	0.443	0.002	11
0.351	0.443	0.002	12
0.401	0.442	0.002	13
0.451	0.441	0.002	14
0.501	0.441	0.001	15
0.551	0.440	0.001	16
0.601	0.439	0.001	17
0.651	0.438	0.001	18
0.701	0.438	0.001	19
0.751	0.437	0.001	20
0.801	0.436	0.001	21
0.851	0.435	0.001	22
0.901	0.435	0.001	23
0.951	0.434	0.001	24

The value of SD changes from about 20% of  $k_{\text{app}}$  to  $<1\%$  from segments 6 to 24.

The  $k_{\text{IRC}}$ -time profile for product formation for the reaction of PNM under these conditions shows an initial value close to  $0.6 \text{ s}^{-1}$ , decreases sharply to about  $0.34 \text{ s}^{-1}$  at about 10 ms, and then rises more slowly to  $0.43 \text{ s}^{-1}$  at about 60 ms and is approximately constant for the remainder of the reaction period analyzed (see Fig. 4).

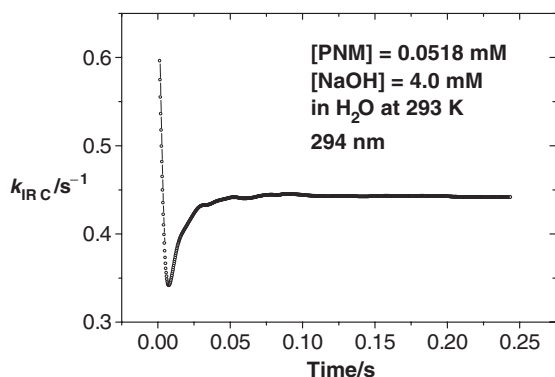


**Figure 4** Apparent IRC ( $k_{\text{IRC}}$ )–time plot for the reaction of PNM (0.052 mM) with hydroxide ion (4.0 mM) in water at 298 (1.0 HL = 1.593 s).

## FORMAL HYDRIDE TRANSFER REACTIONS OF NADH MODELS

### The Reaction of Beta-N-acetyl hexosaminidase (BNAH) with N-Methylacridinium Ion ( $\text{MA}^+$ ) in Acetonitrile

Detailed studies of the reactions of BNAH and analogs with substituted isoquinolinium cations were published by Bunting and coworkers [13a–c] in the early 1980s and were later reviewed [13d].

Conventional pseudo-first-order analysis of the BNAH– $\text{MA}^+$  reaction (Scheme 3) illustrated in Table VII reveals that  $k_{\text{app}}$  varies smoothly from 0.564 for 0.5 HL to 0.502 for the 4 HL analysis, approximately a change of 10% over that range. In this case, reactant ( $\text{MA}^+$ ) decay was monitored at 430 nm and  $k_{\text{app}}$  was equal to 1.553 for segment 1, 0.584 for segment 10, and finally 0.541 for segment 24 (Table VIII). The SD values were large in the early segments and were of the order of 1% of the corresponding  $k_{\text{app}}$  from segment 11 onward.

**Table VII** Changes in the Slopes and the Intercepts with the Extent of Reaction during Conventional Pseudo-First-Order Analysis of the Reaction of BNAH (7.2 mM) with  $\text{MA}^+$  (0.3 mM) in Acetonitrile at 298 K

$k_{\text{app}}$ ( $\text{s}^{-1}$ )	Intercept ( $\text{s}^{-1}$ )	Number of HL
0.564	0.013	0.50
0.536	0.020	1.00
0.522	0.029	2.00
0.513	0.039	3.00
0.502	0.056	4.00

**Table VIII** Apparent Rate Constants and Standard Deviations Obtained by the 24-Point Sequential Analysis of the Reaction of BNAH (7.2 mM) with  $\text{MA}^+$  (0.3 mM) in AN at 298 K

Time (s)	$k_{\text{app}}$ ( $\text{s}^{-1}$ )	SD ( $\text{s}^{-1}$ )	Segment
0.008	1.553	0.574	1
0.012	1.393	0.225	2
0.016	1.236	0.122	3
0.019	1.106	0.118	4
0.023	1.002	0.100	5
0.041	0.795	0.022	6
0.077	0.679	0.015	7
0.113	0.626	0.016	8
0.150	0.599	0.014	9
0.186	0.584	0.011	10
0.222	0.573	0.008	11
0.258	0.567	0.006	12
0.294	0.561	0.005	13
0.331	0.557	0.004	14
0.367	0.555	0.004	15
0.403	0.553	0.004	16
0.439	0.551	0.004	17
0.475	0.549	0.004	18
0.512	0.548	0.004	19
0.548	0.546	0.005	20
0.584	0.545	0.005	21
0.620	0.543	0.006	22
0.656	0.542	0.006	23
0.693	0.541	0.006	24

The  $k_{\text{IRC}}$ –time profile (Fig. 5) has the form expected for reactant decay in a complex mechanism decaying rapidly from an initial value of close to  $2.0 \text{ s}^{-1}$  before approaching a very slowly descending value at times greater than about 1.5 s.

### The Reaction of N-Methyl-9,10-dihydroacridine (MAH) with Tropylium Ion ( $\text{Tr}^+$ ) in Acetonitrile

We are not aware of previous studies of the reaction between MAH and  $\text{Tr}^+$  (Scheme 4). This system has the experimental advantage that  $\text{Tr}^+$  does not absorb above 300 nm, leaving a large wavelength range over which to monitor product ( $\text{MA}^+$ ) formation in acetonitrile.

The conventional pseudo-first-order analysis in this case follows the general pattern that is emerging, a  $k_{\text{app}}$  value of  $0.245 \text{ s}^{-1}$  (1 HL) and decreasing smoothly to  $0.190 \text{ s}^{-1}$  (4 HL). The corresponding intercepts increase from 0.0064 (0.5 HL) to 0.0973 (4 HL), a factor of about 15 indicating a great deal of curvature in the correlation (Table IX).

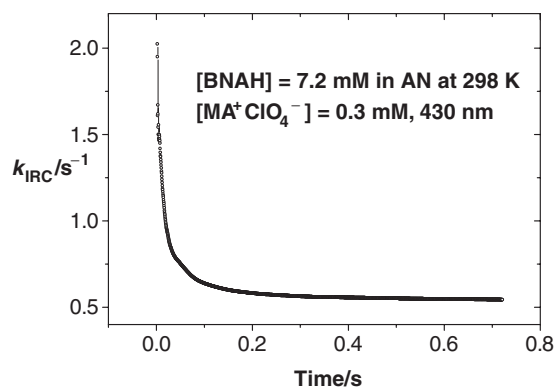
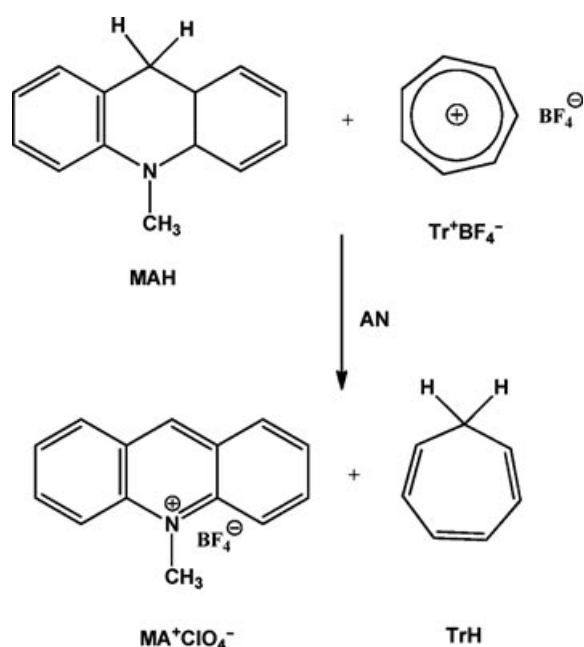
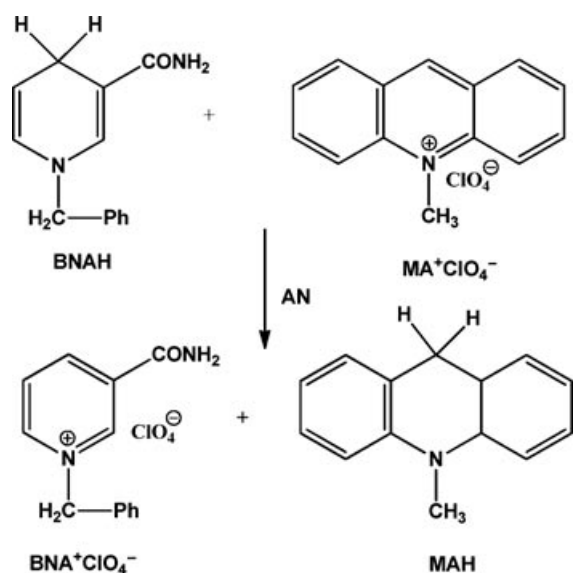


**Figure 5** Apparent IRC ( $k_{IRC}$ )–time plot for the reaction of BNAH (7.2 mM) with  $MA^+$  (0.3 mM) in acetonitrile at 298 K.

**Table IX** Changes in the Slopes and the Intercepts with the Extent of Reaction during Conventional Pseudo-First-Order Analysis of the Reaction of MAH (0.4 mM) with  $Tr^+$  (0.05 M) in Acetonitrile at 298 K

$k_{app}$ ( $s^{-1}$ )	Intercept ( $s^{-1}$ )	Number of HL
0.245	0.0064	0.50
0.225	0.0199	1.00
0.206	0.0499	2.00
0.190	0.0973	3.00

The 24-point sequential analysis for product evolution ( $MA^+$ ) in this case, once again a sharply decreasing  $k_{app}$  from 0.699 at segment 1 to a more slowly decreasing 0.266  $s^{-1}$  at segment 8 and finally at segment 24,  $k_{app}$  equals 0.222  $s^{-1}$  (Table X).

**Table X** Apparent Rate Constants and Standard Deviations Obtained by the 24-Point Sequential Analysis of the Reaction of MAH (0.2 mM) with  $Tr^+$  (50 mM) in Acetonitrile at 298 K

Time (s)	$k_{app}$ ( $s^{-1}$ )	SD ( $s^{-1}$ )	Segment
0.014	0.699	0.027	1
0.026	0.563	0.014	2
0.039	0.488	0.009	3
0.051	0.442	0.008	4
0.064	0.407	0.007	5
0.126	0.326	0.005	6
0.251	0.281	0.003	7
0.376	0.266	0.002	8
0.501	0.258	0.002	9
0.626	0.252	0.002	10
0.751	0.248	0.002	11
0.876	0.245	0.001	12
1.001	0.242	0.001	13
1.126	0.239	0.001	14
1.251	0.237	0.001	15
1.376	0.235	0.001	16
1.501	0.233	0.001	17
1.626	0.231	0.001	18
1.751	0.229	0.001	19
1.876	0.228	0.001	20
2.001	0.226	0.001	21
2.126	0.225	0.001	22
2.251	0.223	0.001	23
2.376	0.222	0.001	24

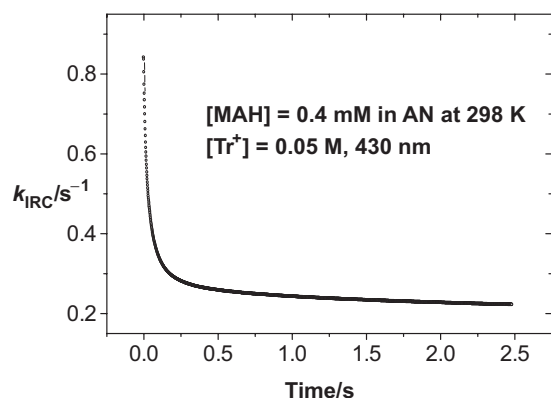


**Figure 6** Apparent IRC ( $k_{\text{IRC}}$ )–time plot for the reaction of MAH (0.4 mM) with  $\text{Tr}^+$  (50 mM) in acetonitrile at 298 K (1.0 HL = 2.87 s).

The  $k_{\text{IRC}}$ –time profile (Fig. 6) allows for a more detailed illustration of the pattern indicated above. It should be pointed out, once again, that this general pattern is obviously inconsistent with a one-step mechanism and that there is an intermediate that absorbs at the wavelength of the experiment.

### The Reaction of 1-Benzyl-3-cyanoquinolinium Ion ( $\text{BQCN}^+$ ) with *N*-Methyl-9,10-dihydroacridine in Acetonitrile

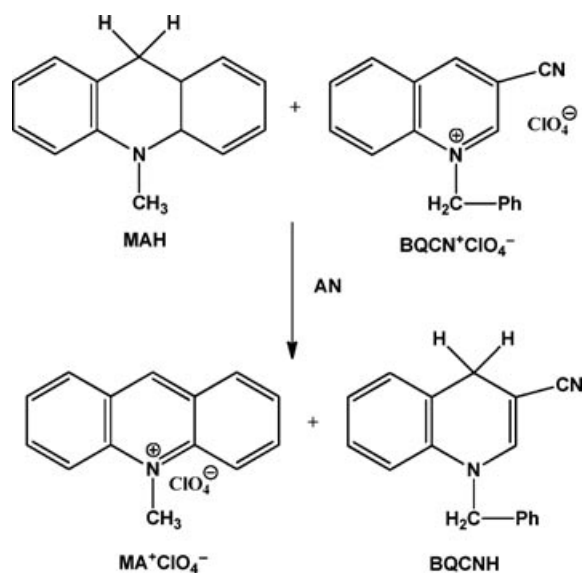
The reaction between MAH and  $\text{BQCN}^+$  in AN (Scheme 5) has been considered to be an authentic example of a direct hydride transfer reaction mainly due to the work of Kreevoy and coworkers [14]. We presented an alternative three-step mechanism in 2003 [15], which was challenged by Perrin and Zhao in 2008 [16]. The mechanism has been found to be even more complex than we first believed [15] and was shown to involve an oxygen-catalyzed chain reaction even when carried out in a glove box under a nitrogen atmosphere [7].

The data presented here are for the reaction between MAH (40 mM) with  $\text{BQCN}^+$  (0.5 mM) in acetonitrile half-saturated with air (Table XI). The latter was achieved by mixing the MAH solution from which air was removed from a  $\text{BQCN}^+$  solution in acetonitrile saturated with air. The 24-point sequential analysis in this case is distinctively different from any previously presented. In Table XII, we see that  $k_{\text{app}}$  first increases to a maximum value ( $0.000866 \text{ s}^{-1}$ ) before decreasing slowly to  $0.000831 \text{ s}^{-1}$  at segment 8 and then increases smoothly for the remainder of the time period analyzed with a value of  $0.001356 \text{ s}^{-1}$  at segment 24.

The  $k_{\text{IRC}}$ –time profile (Fig. 7) shows an important detail only hinted at in Table XII. In Fig. 7, we see

**Table XI** Changes in the Slopes and the Intercepts with the Extent of Reaction during Conventional Pseudo-First-Order Analysis of the Reaction of MAH (40 mM) with  $\text{BQCN}^+$  (0.5 mM) in Acetonitrile at 298 K

$k_{\text{app}} (\text{s}^{-1})$	Intercept ( $\text{s}^{-1}$ )	Number of HL
0.00095	−0.029	0.50
0.00116	−0.066	1.00
0.00148	−0.152	2.00
0.00171	−0.241	3.00
0.00186	−0.312	4.00



**Scheme 5**

an initial sharp increase in  $k_{\text{IRC}}$  from the initial to a maximum value nearly 50% greater than the former. From the maximum,  $k_{\text{IRC}}$  first decreased slightly and then began a steady increase for the remainder of the analysis period.

### $\text{S}_{\text{N}}2$ REACTIONS OF ALKYL HALIDES WITH ANIONIC AND NEUTRAL NUCLEOPHILES

#### The Reaction of Bromoacetonitrile with Phenoxide Ion in Acetonitrile

Bromoacetonitrile ( $\text{BrCN}$ ) is not a common alkyl halide, but  $\text{ClCN}$  has been used in recent publications concerned with the mechanism of the  $\text{S}_{\text{N}}2$  reaction [17]. The advantage of studying  $\text{S}_{\text{N}}2$  reactions of  $\text{BrCN}$  is that it is much more reactive than a typical alkyl halide.

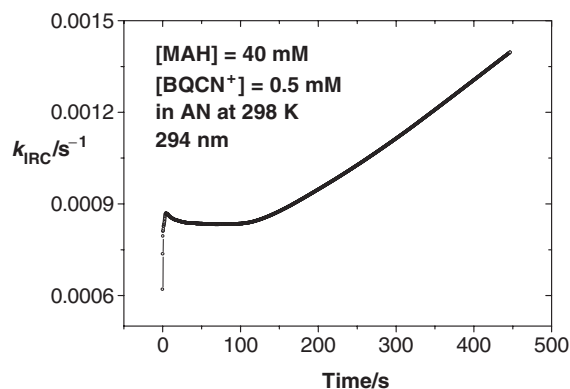
The data for the conventional pseudo-first-order analysis of the reaction (Scheme 6) illustrated in

**Table XII** Apparent Rate Constants and Standard Deviations Obtained by the 24-Point Sequential Analysis of the Reaction of MAH (40 mM) with BQCN<sup>+</sup> (0.5 mM) in Acetonitrile at 298 K

Time (s)	$k_{app}$ (s <sup>-1</sup> )	SD (s <sup>-1</sup> )	Segment
2.5	0.000830	0.00003	1
4.7	0.000866	0.00001	2
7.0	0.000865	0.00001	3
9.2	0.000859	0.00001	4
11.5	0.000854	0.00001	5
22.7	0.000842	0.00001	6
45.2	0.000834	0.00001	7
67.7	0.000831	0.00001	8
90.2	0.000832	0.00000	9
112.7	0.000838	0.00000	10
135.2	0.000856	0.00000	11
157.7	0.000883	0.00001	12
180.2	0.000914	0.00001	13
202.7	0.000948	0.00001	14
225.2	0.000983	0.00001	15
247.7	0.001020	0.00001	16
270.2	0.001058	0.00001	17
292.7	0.001097	0.00002	18
315.2	0.001138	0.00002	19
337.7	0.001181	0.00002	20
360.2	0.001224	0.00002	21
382.7	0.001268	0.00002	22
405.2	0.001312	0.00003	23
427.7	0.001356	0.00003	24

Table XIII conform to the pattern observed in earlier tables with  $k_{app}$  equal to 0.0350 s<sup>-1</sup> (0.5 HL) and decreasing smoothly to 0.0289 s<sup>-1</sup> (4 HL).

In segment 1 of the 24-point sequential analysis (Table XIV),  $k_{app}$  for reactant (PO<sup>-</sup>) decay was equal

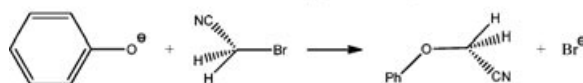
**Figure 7** Apparent IRC ( $k_{IRC}$ )-time plot for the reaction of MAH (40 mM) with BQCN<sup>+</sup> (0.5 mM) in acetonitrile at 298 K (1.0 HL = 602 s).**Table XIII** Changes in the Slopes and the Intercepts with the Extent of Reaction during Conventional Pseudo-First-Order Analysis of the Reaction of BrAN (5.0 mM) with PO<sup>-</sup> (0.50 mM) in Acetonitrile at 298 K

$k_{app}$ (s <sup>-1</sup> )	Intercept (s <sup>-1</sup> )	Number of HL
0.0350	0.0125	0.50
0.0346	0.0134	1.00
0.0336	0.0244	2.00
0.0318	0.0565	3.00
0.0289	0.1353	4.00

**Table XIV** Apparent Rate Constants and Standard Deviations Obtained by the 24-Point Sequential Analysis of the Reaction of BrAN (5.0 mM) with PO<sup>-</sup> (0.50 mM) in Acetonitrile at 298 K

Time (s)	$k_{app}$ (s <sup>-1</sup> )	SD (s <sup>-1</sup> )	Segment
0.059	0.1038	0.0188	1
0.113	0.0841	0.0139	2
0.167	0.0687	0.0089	3
0.220	0.0598	0.0059	4
0.274	0.0542	0.0039	5
0.543	0.0426	0.0012	6
1.080	0.0382	0.0005	7
1.618	0.0369	0.0005	8
2.156	0.0364	0.0005	9
2.693	0.0361	0.0004	10
3.231	0.0359	0.0004	11
3.768	0.0358	0.0004	12
4.306	0.0357	0.0004	13
4.844	0.0356	0.0004	14
5.381	0.0355	0.0003	15
5.919	0.0355	0.0003	16
6.456	0.0354	0.0003	17
6.994	0.0354	0.0003	18
7.532	0.0353	0.0003	19
8.069	0.0352	0.0003	20
8.607	0.0352	0.0003	21
9.144	0.0351	0.0003	22
9.682	0.0351	0.0003	23
10.220	0.0350	0.0003	24

to 0.1038 s<sup>-1</sup> with an SD of 0.0188. Both quantities decreased sharply to 0.0382 and 0.0005 s<sup>-1</sup>, respectively, in segment 7. The trend continued but with much smaller changes for the remainder of the reaction period.

**Scheme 6**

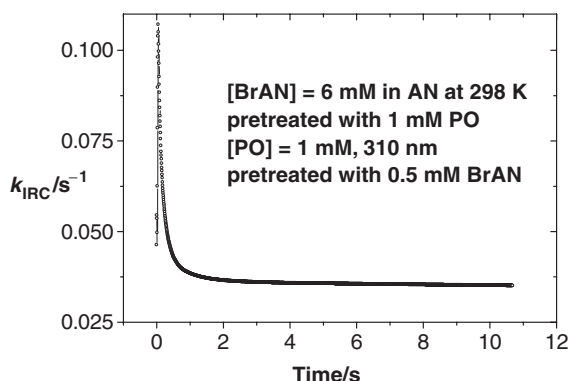


**Figure 8** Apparent IRC ( $k_{\text{IRC}}$ )-time plot for the reaction of BrAN (5.0 mM) with  $\text{PO}^-$  (0.50 mM) in acetonitrile at 298 K (1.0 HL = 19.0 s).

The  $k_{\text{IRC}}$ -time profile (Fig. 8) shows an initial steep rise to a maximum at short times before decreasing toward a very slightly decreasing or nearly constant value.

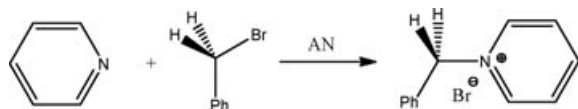
### The Reaction of Pyridine with Benzyl Bromide in Acetonitrile

The pseudo-first-order analysis data of the reaction of pyridine with benzyl bromide (Scheme 7) in Table XV fit the pattern in correlation quantities expected for product evolution in a complex mechanism. It would appear from the  $k_{\text{app}}$  values that a steady state may be approached late in the reaction.

The data from the 24-point sequential analysis presented in Table XVI show some deviation from the picture presented by the data in Table XV taken alone.

**Table XV** Changes in the Slopes and the Intercepts with the Extent of Reaction during Conventional Pseudo-First-Order Analysis of the Reaction of Pyridine (1.25 M) with Benzyl Bromide (40.0 mM) in Acetonitrile at 298 K

$k_{\text{app}}$ ( $\text{s}^{-1}$ )	Intercept ( $\text{s}^{-1}$ )	Number of HL
0.00079	-0.024	0.50
0.00094	-0.052	1.00
0.00104	-0.086	2.00
0.00109	-0.113	3.00
0.00112	-0.134	4.00
0.00114	-0.152	5.00



**Scheme 7**

**Table XVI** Apparent Rate Constants and Standard Deviations Obtained by the 24-Point Sequential Analysis of the Reaction of Pyridine (1.25 M) with Benzyl Bromide (40.0 mM) in Acetonitrile at 298 K

Time (s)	$k_{\text{app}}$ ( $\text{s}^{-1}$ )	SD ( $\text{s}^{-1}$ )	Segment
2.34	0.000174	0.00023	1
4.46	0.000126	0.00020	2
6.59	0.000117	0.00014	3
8.71	0.000128	0.00011	4
10.84	0.000147	0.00008	5
21.46	0.000243	0.00004	6
42.71	0.000381	0.00002	7
63.96	0.000479	0.00002	8
85.21	0.000557	0.00002	9
106.46	0.000620	0.00003	10
127.71	0.000674	0.00003	11
148.96	0.000721	0.00003	12
170.21	0.000769	0.00004	13
191.46	0.000809	0.00005	14
212.71	0.000840	0.00006	15
233.96	0.000869	0.00007	16
255.21	0.000896	0.00008	17
276.46	0.000922	0.00008	18
297.71	0.000947	0.00009	19
318.96	0.000971	0.00010	20
340.21	0.000994	0.00011	21
361.46	0.001018	0.00012	22
382.70	0.001042	0.00013	23
403.95	0.001066	0.00014	24

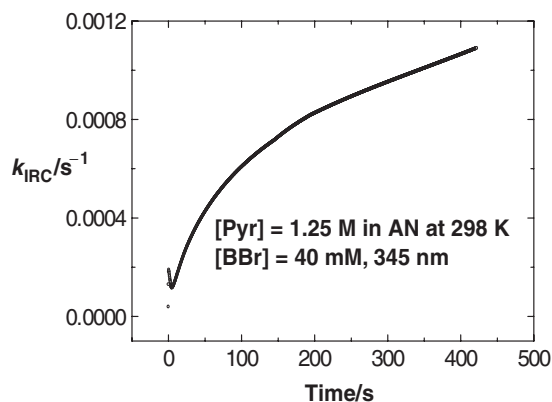


**Figure 9** Apparent IRC ( $k_{\text{IRC}}$ )-time plot for the reaction of pyridine (1.25 M) with benzyl bromide in acetonitrile at 298 K (1.0 HL = 697 s).

The first three segments show that  $k_{\text{app}}$  first decreases sharply before beginning the slower rise toward a possible steady-state value.

The  $k_{\text{IRC}}$ -time profile for the  $\text{S}_{\text{N}}2$  reaction between benzyl bromide and pyridine (Fig. 9) indicates a possible further complication; after the initial small value at point 1, a maximum is observed at point 4 ( $k_{\text{IRC}} = 0.000188$ ) before the  $k_{\text{app}}$  decay indicated in Table XVI.

## CONCLUSIONS

Experimental absorbance time profiles obtained from eight different fundamental organic reactions were processed using three different nonconventional pseudo-first-order kinetic procedures, and the results are summarized. The objective of the presentation has been to allow the readers to make their own conclusions regarding the mechanistic significance of the data without the distraction of the author's conclusions.

The procedures include (1) HL dependence of  $k_{app}$  during convention pseudo-first-order analysis, (2) sequential linear pseudo-first-order correlation, and (3) revised IRC analysis. Using these procedures, the determination as to whether a reaction follows a simple one step or a more complex mechanism can be made using a minimum of both time and materials. This, of course, is only the first step in the investigation of the mechanism of a reaction and should be followed by experiments under all applicable conditions, including changes in reactant concentrations, wavelengths at which absorbance–time data are obtained, temperature, and isotopic composition of reactants to name the most common variables.

## BIBLIOGRAPHY

- Hammond, G. S. *Pure Appl Chem* 1997, 69, 1919–1922.
- Hammett, L. P. *Physical Organic Chemistry*, 2nd ed.; McGraw-Hill: New York, 1970.
- Moore, J. W.; Pearson, R. G. *Kinetics and Mechanism*, 3rd ed.; Wiley: New York, 1981.
- (a) Nagy, T.; Turányi, T. *Int J Chem Kinet* 2011, 43, 359–378; (b) Kormányos, B.; Horváth, A. K.; Peintler, G.; Nagypál, I. *J Phys Chem A* 2007, 111, 8104–8109; (c) Bandstra, J. Z.; Tratnyek, P. G. *J Math Chem* 2005, 37, 409–422; (d) Vidaurre, G.; Vasquez, V. R.; Whiting, W. B. *Ind Eng Chem Res* 2004, 43, 1395–1404.
- Parker, V. D.; Li, Z.; Handoo, K. L.; Hao, W.; Cheng, J.-P. *J Org Chem* 2011, 76, 1250–1256.
- Li, Z.; Cheng, J.-P.; Parker, V. D. *Org Biomol Chem* 2011, 9, 4563–4569.
- Hao, W.; Parker, V. D. Unpublished work.
- Parker, V. D. *J Phys Org Chem* 2006, 19, 714–724.
- Kresge, A. J. *Can J Chem* 1975, 52, 1897–1903.
- (a) Bernasconi, C. F.; Kliner, D. A. V.; Mullin, A. S.; Ni, J. X. *J Org Chem* 1988, 53, 3342–3351; (b) Bernasconi, C. F.; Ni, J.-X. *J Org Chem* 1994, 59, 4910–4916.
- (a) Bernasconi, C. F.; Wenzel, P. J. *J Org Chem* 2010, 75, 8422–8434; (b) Bernasconi, C. F.; Pérez-Lorenzo, M.; Brown, S. D. *J Org Chem* 2007, 72, 4416–4423; (c) Bernasconi, C. F.; Ali, M.; Gunter, J. C. *J Am Chem Soc* 2003, 125, 151–157; (d) Bernasconi, C. F.; Wenzel, P. J. *J Org Chem* 2003, 68, 6870–6879.
- Ando, K.; Shimazu, Y.; Seki, N.; Yamataka, H. *J Org Chem* 2011, 76, 3937–3945.
- (a) Bunting, J. W.; Sindhuatmadja, S. *J Org Chem* 1981, 46, 4211–4219; (b) Bunting, J. W.; Chew, V. S. F.; Chu, G. *J Org Chem* 1982, 47, 2303–2307; (c) Bunting, J. W.; Chew, V. S. F.; Chu, G. *J. Org. Chem* 1982, 47, 2308–2312; (d) Bunting, J. W. *Bioorg Chem* 1991, 19, 456–491.
- (a) Kim, Y.; Trular, D. G.; Kreevoy, M. M. *J Am Chem Soc* 1991, 113, 7837–7847; (b) Kotchevar, A. T.; Kreevoy, M. M. *J Phys Chem* 1991, 95, 10345–10350; (c) Kreevoy, M. M.; Kotchevar, A. T. *J Am Chem Soc* 1990, 112, 3579–3583; (d) Kreevoy, M. M.; Ostovic, D.; Lee, I. S. H.; Binder, D. A.; King, G. W. *J Am Chem Soc* 1988, 110, 524–530; (e) Ostovic, D.; Lee, I. S. H.; Roberts, R. M. G.; Kreevoy, M. M. *J Org Chem* 1985, 50, 4206–4211; (f) Kreevoy, M. M.; Lee, I. S. H. *J Am Chem Soc* 1984, 106, 2550–2553.
- Lu, Y.; Zhao, Y.; Handoo, K. L.; Parker, V. D. *Org Biomol Chem* 2003, 1, 173–181.
- Perrin, C. L.; Zhao, C. *Org Biomol Chem* 2008, 6, 3349–3353.
- (a) Vayner, G.; Houk, K. N.; Jorgensen, W. L.; Brauman, J. I. *J Am Chem Soc* 2004, 126, 9054–9058; (b) Chen, X.; Regan, C. K.; Craig, S. L.; Krenske, E. H.; Houk, K. N.; Jorgensen, W. L.; Brauman, J. I. *J Am Chem Soc* 2009, 131, 16162–16170, and references cited.